Journal of Alloys and Compounds 499 (2010) 140–143

Contents lists available at ScienceDirect

Journal of Alloys and Compounds

journal homepage: www.elsevier.com/locate/jallcom

Magneto-thermal and magneto-transport behavior around the martensitic transition in $Ni_{50-x}Co_xMn_{40}Sb_{10}$ ($x = 9$, 9.5) Heusler alloys

Ajaya K. Nayak[a], N.V. Rama Rao[a,b], K.G. Suresh[a,*], A.K. Nigam[c]

[a] Magnetic Materials Laboratory, Department of Physics, Indian Institute of Technology Bombay, Powai, Mumbai-400076, India
[b] Defence Metallurgical Research Laboratory, Hyderabad-500058, India
[c] Tata Institute of Fundamental Research, Homi Bhabha Road, Mumbai-400005, India

ARTICLE INFO

Article history:
Received 10 January 2010
Received in revised form 21 March 2010
Accepted 25 March 2010
Available online 2 April 2010

Keywords:
Heusler alloy
Magnetocaloric effect
Magnetoresistance
Martensitic transition

ABSTRACT

The structural, magnetic, magnetocaloric and magnetoresistance behavior in $Ni_{50-x}Co_xMn_{40}Sb_{10}$ ($x = 9$ and 9.5) has been studied around the magnetostructural transition. The X-ray diffraction results at room temperature show that the compound with $x = 9$ is predominantly martensitic whereas the one with $x = 9.5$ is austenite in nature. The maximum magnetic entropy change of 9.2 J kg^{-1} K^{-1} was achieved in $x = 9.5$ at 246 K in a field of 50 kOe and a value of 8.2 J kg^{-1} K^{-1} was found near room temperature for $x = 9$. The effective refrigeration capacity of 106 J/kg has been calculated for $x = 9$, which is larger than the same observed in other Ni–Mn based Heusler alloy systems. A large magnetoresistance of 25% was obtained around room temperature for $x = 9$. The large difference in the magnetization between the martensitic and austenite phases is responsible for the large magnetocaloric effect and magnetoresistance in these compounds.

1. Introduction

It is observed that materials undergoing magnetostructural transition exhibit many interesting properties, as there is a large change in the magnetic properties that occurs at the structural transition. The most interesting candidates in this category are Ni–Mn based ferromagnetic Heusler alloys. After the discovery of large magnetic field-induced strain in Ni–Mn–Ga by Ullakko et al. [1], Heusler alloys have received considerable attention for their multifunctional applications in various fields. In recent studies the magnetostructural transition has been reported in many Heusler alloy systems such as Ni–Mn–X (X = Ga, Sn, In, Sb) [2–5]. These alloys undergo a structural transition from high magnetic austenite phase to a considerably low magnetic martensitic phase. Owing to this change in magnetization around the martensitic transition, a large magnetocaloric effect and magnetoresistance are obtained [2,6–12]. A large magnetic field-induced shape memory effect has been found in $Ni_{45}Co_5Mn_{36.7}In_{11.3}$ single crystals [12]. Similar magnetic and magnetocaloric properties have been reported in Ni–Co–Mn–Sn [13], Ni–Co–Mn–Ga [14] and Ni–Co–Mn–Sb [15] systems.

Recently, several studies have been reported on the magnetostructural and magneto-thermal properties of Ni–Mn–Sb Heusler system [5,9,15–17]. In a very recent work, Nayak et al. have reported that $Ni_{50-x}Co_xMn_{38}Sb_{12}$ shows a large magnetic entropy change (ΔS_M) and enhanced exchange bias behavior [15,18]. It was also reported that the martensitic transition temperature can be tuned remarkably by application of field as well as pressure [19]. However, in most of the Heusler alloy systems, including the one studied by us, the width of the ΔS_M vs. T is very narrow, which gives rise to low refrigeration capacity (RC). It can be mentioned that refrigeration capacity is one of the quality factors characterizing a magnetic refrigerant. RC is defined as the area under the full width at half maximum in ΔS_M vs. T curve. In the present study we observed that by suitable adjustment of Ni and Co concentrations, a large RC can be achieved at room temperature. Also we found that the hysteresis loss, which is undesirable, has been considerably reduced. In addition, we have also measured the magnetoresistance around the martensitic transition temperature.

2. Experimental details

Polycrystalline $Ni_{50-x}Co_xMn_{40}Sb_{10}$ ($x = 9$, 9.5) alloys were prepared by arc-melting the stoichiometric amounts of Ni, Co, Mn, Sb of at least 99.99% purity in high pure argon atmosphere. The ingots were re-melted several times to get good homogeneity and were subsequently annealed in evacuated quartz tubes at 850 °C for 24 h. The structural characterization of the materials was done by powder X-ray diffractograms (XRD) using Cu-Kα radiation. The magnetization measurements were carried out using a vibrating sample magnetometer attached to a Physical Property Measurement System (Quantum Design, PPMS-6500). The resistivity measurements were done by the four-probe method using PPMS. The differential scanning calorimetry (DSC) measurements were performed using the TA Q100 setup with a cooling/heating rate of 20 K min^{-1}.

* Corresponding author.
E-mail address: suresh@phy.iitb.ac.in (K.G. Suresh).

0925-8388/$ – see front matter © 2010 Elsevier B.V. All rights reserved.
doi:10.1016/j.jallcom.2010.03.190

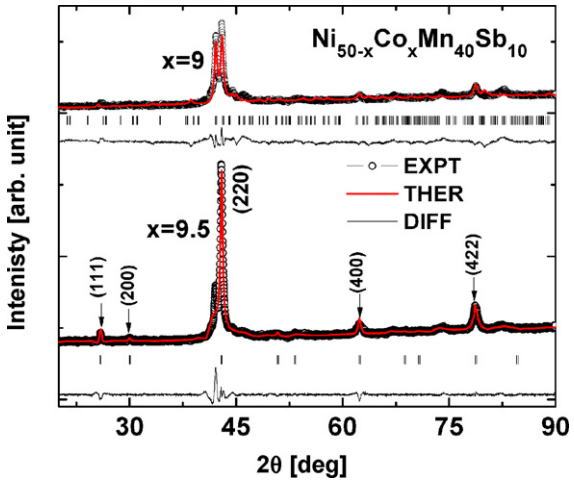

Fig. 1. The X-ray diffraction patterns of $Ni_{50-x}Co_xMn_{40}Sb_{10}$ (x = 9, 9.5) along with the Rietveld refinement. The plots at the bottom show the difference between the experimental and the theoretical patterns.

3. Results and discussion

The X-ray diffraction patterns at room temperature, along with the Rietveld refinement for the two alloys are shown in Fig. 1. The refinement for alloy with x = 9 shows martensitic phase (orthorhombic, space group – Pmma, lattice parameter – a = 8.38 Å, b = 5.76 Å, c = 4.11 Å), whereas the one with x = 9.5 shows austenite phase (cubic, space group – Fm3m, lattice parameter – a = b = c = 5.95 Å) at room temperature. For x = 9.5 the existence of a small peak near the (2 2 0) austenite peak indicates the presence of a very small amount of martensitic phase. This is because the alloy possesses a high temperature austenite phase which is transformed to low temperature martensitic phase around room temperature. The details of the phase transition from austenite to martensitic phase have been reported in similar types of compounds elsewhere [15,18].

Fig. 2 shows the DSC studies for the alloys with x = 9 and 9.5. The temperature vs. heat flow measurements were performed in both heating and cooling modes. In the heat flow curve the vertical displacements (peaks) are proportional to the heat capacity of the sample and is expected to change with composition. The start and finish of the transition temperatures are taken at the temperature where the heat flux curve starts changing the slope. In the cooling curve the start and finish points indicate the martensitic start (M_S) and martensitic finish temperatures (M_F). Similarly in heating

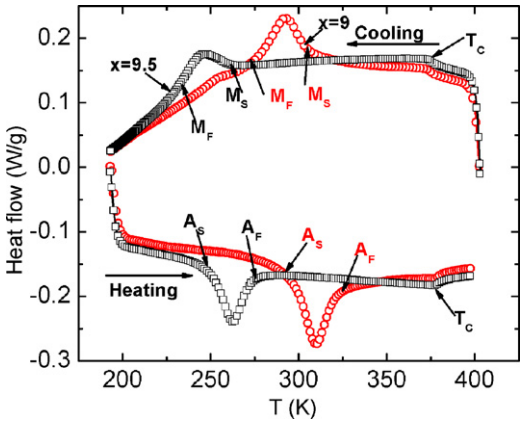

Fig. 2. Heat flow as a function of temperature in $Ni_{50-x}Co_xMn_{40}Sb_{10}$ (x = 9 and 9.5), both in cooling and heating modes.

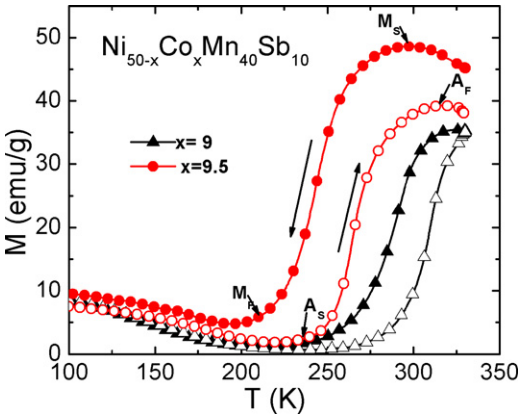

Fig. 3. The field cool cooling (FCC) and field cool warming (FCW) magnetization data as a function of temperature for $Ni_{50-x}Co_xMn_{40}Sb_{10}$.

curve, the start and finish points indicate the austenite start (A_S) and austenite finish (A_F) temperatures. The martensitic transition temperature is defined as $T_M = (M_S + M_F)/2$ and the austenite transition temperature as $T_A = (A_S + A_F)/2$. For x = 9, the various transition temperatures obtained from DSC are M_S = 304 K, M_F = 270 K, A_S = 296 K, A_F = 324 K and for x = 9.5, the corresponding values are M_S = 262 K, M_F = 232 K, A_S = 250 K, A_F = 276 K. From these data, it has been calculated that T_M = 291 K, T_A = 310 K for x = 9 and T_M = 247 K, T_A = 263 K for x = 9.5. The transition temperatures obtained from the DSC are in very good agreement with those obtained from the magnetization data.

The temperature dependence of magnetization around the martensitic transition is shown in Fig. 3. The measurements have been performed in two different modes. In the field cooled cooling (FCC) mode, the data was collected during the cooling in field, while in the field cooled warming (FCW) mode, the data was collected while heating, after field cooling. In both the cases, the cooling and the measuring fields were 1 kOe. There are two types of transitions expected in these materials. The ferromagnetic–paramagnetic transition of the austenite phase is not shown in Fig. 3 as it occurs above 330 K. As the temperature decreases below 330 K, the magnetization initially goes through a maximum value and then decreases drastically. The temperature corresponding to the maximum magnetization value is called the martensitic start (M_S) and that of minimum value called the martensitic finish temperature (M_F), as indicated in the FCC curve of x = 9.5. In the FCW curve the minimum magnetization point is called the austenite start temperature (A_S) and the maximum point is called the austenite finish temperature (A_F). In the M_F–A_F temperature regime, a mixture of austenite and martensitic phase is expected. The difference between FCC and FCW curves reflects the thermal hysteresis associated with the first order structural transition. The sharp decrease in magnetization below M_S indicates the presence of some non-ferromagnetic component in the M_S–M_F regime. It is expected that in the entire martensitic region, there is a coexistence of both FM and AFM components. In the off-stoichiometric $Ni_{50-x}Co_xMn_{40}Sb_{10}$ alloys the extra Mn atoms occupy the Sb sites. The Mn–Mn distance between the Mn atoms occupying the Mn and Sb sites decreases after the martensitic transition, which introduces an antiferromagnetic component in the martensitic phase [20].

The isothermal magnetization curves taken at 2 K intervals around the martensitic transition temperature for $Ni_{41}Co_9Mn_{40}Sb_{10}$ and $Ni_{40.5}Co_{9.5}Mn_{40}Sb_{10}$ are shown in Fig. 4. In Fig. 4(a) both the increasing and the decreasing field data are shown, whereas in Fig. 4(b) only the increasing field data is shown. The inset of Fig. 4(a) shows the hysteresis loss for the compound with x = 9. The upward nature of the M–H isotherms (in Fig. 4(a))

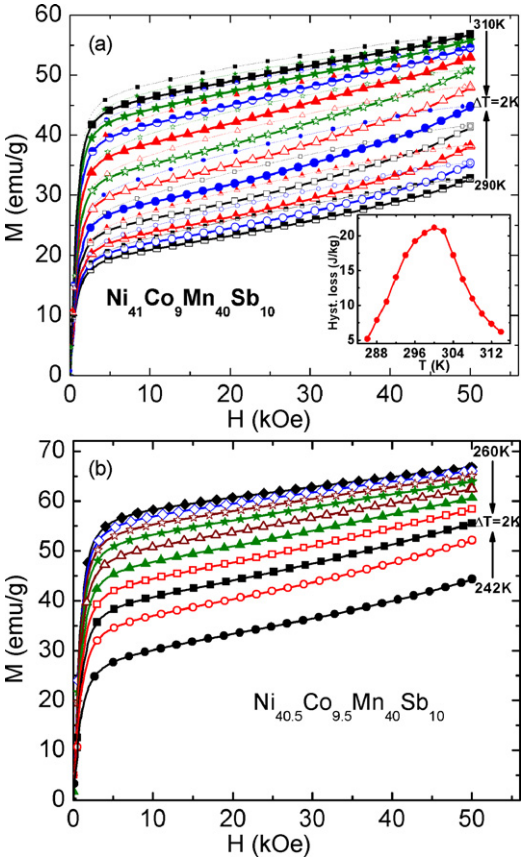

Fig. 4. (a) Isothermal magnetization $M(H)$ curves around the martensitic transition temperature for $Ni_{41}Co_9Mn_{40}Sb_{10}$. The solid line represents the increasing field data and the dotted line indicates the decreasing field data. (b) $M(H)$ curves for $Ni_{40.5}Co_{9.5}Mn_{40}Sb_{10}$. The inset of (a) shows the variation of hysteresis loss with temperature.

starting just below 50 kOe is an indication of the metamagnetic transition. The first order nature of this transition can be seen from the $M^2 \sim H/M$ (Arrott) plots shown in Fig. 5. The metamagnetic character of the M–H isotherms is due to the field-induced reverse martensitic transformation from a low magnetization martensitic state to a higher magnetization austenite state. The S-shaped Arrott plots clearly suggest that the metamagnetic transition is of first order in nature.

The magnetocaloric effect (ΔS_M) was calculated from the isothermal magnetization curves obtained in intervals of 2 K

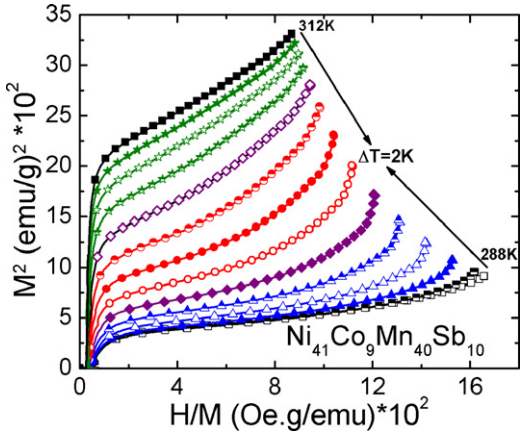

Fig. 5. Arrott plots for $Ni_{41}Co_9Mn_{40}Sb_{10}$, showing the first order nature of transition.

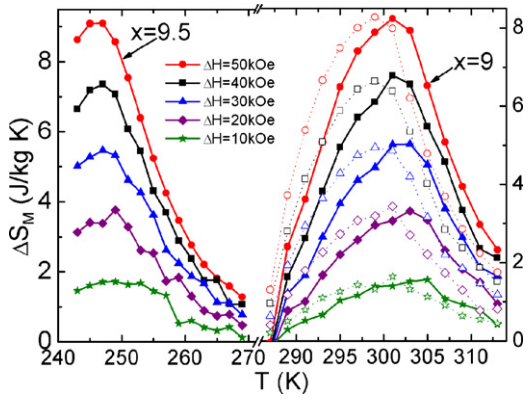

Fig. 6. Magnetic entropy change (ΔS_M) as a function of temperature in $Ni_{50-x}Co_xMn_{40}Sb_{10}$ ($x = 9, 9.5$). In $x = 9$ the filled symbols represent ΔS_M calculated from increasing field data and the open symbols correspond to the decreasing field data.

around the martensitic transition and using the Maxwell's relation given by

$$\Delta S_M(T, H) = \int_0^H \left(\frac{\partial M(T, H)}{\partial T}\right)_H dH \quad (1)$$

Since we used a constant temperature interval, Eq. (1) can be written as

$$\Delta S_M \approx \frac{1}{\Delta T}\left[\int_0^H (M(T + \Delta T, H) - M(T, H))dH\right] \quad (2)$$

The refrigeration capacity was calculated using the relation

$$RC = \int_T^{T_2} (\Delta S_M(T))_{\Delta H} dT \quad (3)$$

where T_1 and T_2 are the temperatures of the cold and the hot sinks.

Fig. 6 shows the variation of ΔS_M with temperature in various applied field for $x = 9$ and 9.5. ΔS_M of 9.2 J kg^{-1} K^{-1} is obtained around 245 K for $x = 9.5$ and a value of 8.2 J kg^{-1} K^{-1} at room temperature for $x = 9$. These values are larger than the value reported in Ni–Mn–Sb system [16]. The refrigeration capacity is calculated by integrating $\Delta S_M(T)$ curve over the temperature span corresponding to the full width at half maximum (FWHM) points. The RC values obtained for $x = 9$ is 120 J/kg. The average hysteresis loss is estimated to be 14 J/kg for the same temperature interval used for calculating the RC and this is subtracted from RC to get the effective refrigeration capacity of 106 J/kg. This value of RC is much larger than that obtained in other Ni–Mn–Sb alloys as well as many other Heusler alloy systems [6,9,16]. The present observation is even more interesting as the large RC value occurs at room temperature.

The fact that the martensitic transition temperature can be tuned by suitable adjustment of Co/Ni concentration along with the observation of large RC over the room temperature make this system quite interesting from the application point of view. The large magnetic entropy change is related to the strong magnetostructural coupling giving rise to a large value of $(\partial M/\partial T)$. In general, the Ni–Mn based Heusler alloys have different magnetic states in martensitic and austenite phases. The low magnetization martensitic state can be tuned to high magnetization austenite state by application of field as well as temperature. Therefore, one gets a large difference between two consecutive magnetization isotherms and consequently a large ΔS_M.

Fig. 7(a) shows the variation of resistivity with temperature for $Ni_{41}Co_9Mn_{40}Sb_{10}$. The variation of resistivity with temperature is constant until the temperature reaches the martensitic transition region. Near the martensitic transition it drops abruptly to nearly half of its previous value and then increases slightly with further

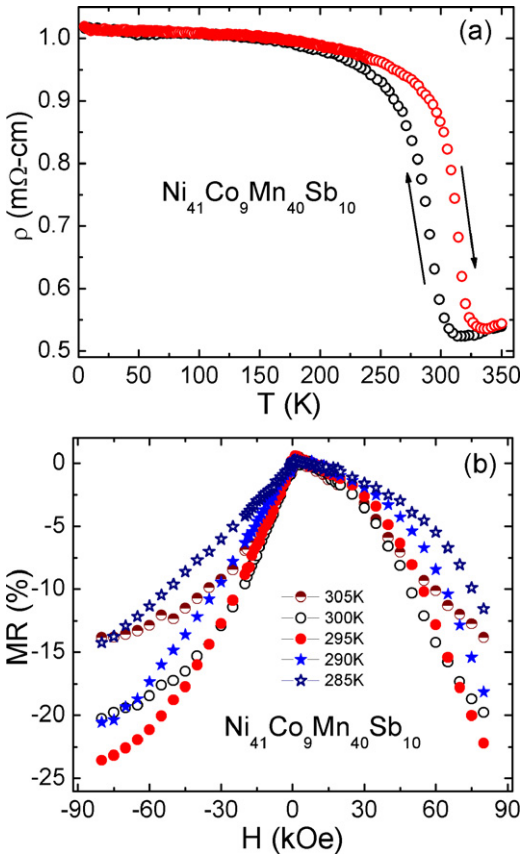

Fig. 7. (a) Temperature variation of resistivity for $Ni_{41}Co_9Mn_{40}Sb_{10}$ measured in zero field, (b) field dependence of magnetoresistance at various temperatures.

increase in temperature. The first order nature of the structural transition is clearly reflected from the hysteresis between the cooling and heating data. It is observed that field can remarkably reduce the martensitic transition temperature [15]. A large magnetoresistance is expected in the same temperature range over which the applied magnetic field can induce the transformation. Fig. 7(b) shows the variation of magnetoresistance with field at various temperatures for $Ni_{41}Co_9Mn_{40}Sb_{10}$. The measuring temperatures were achieved by cooling the sample from 330 K. Once the desired temperature was achieved, the measurement was carried out by varying the field from −80 kOe to +80 kOe. The curves are found to be asymmetric for the positive and negative fields. This may be due to the variations in the relative concentrations of martensitic and austenite phases (in this mixed phase region) as negative and positive fields are applied. Supercooling/superheating associated with the first order transition must be responsible for this asymmetry [21]. The magnetoresistance value is found to be very large, about 25%, in a field of 80 kOe, around room temperature.

4. Conclusions

In conclusion, we have studied the magnetic, magnetocaloric and magnetoresistance behavior of $Ni_{50-x}Co_xMn_{40}Sb_{10}$ ($x = 9$ and 9.5) around the martensitic transition temperature. By suitable adjustment of Co/Ni composition, a large magnetocaloric effect and magnetoresistance have been achieved around room temperature. Strong magnetostructural coupling with large $\partial M/\partial T$ is responsible for the large entropy change and magnetoresistance. The observation of large refrigerant capacity is due to the spreading of ΔS_M curve over a larger temperature interval, which is attributed to the continuous nature of the martensitic transition. The results obtained in this study seem to be very promising as far as the multifunctional applications of Heusler alloys are concerned.

References

[1] K. Ullakko, J.K. Huang, C. Kantner, R.C. O'Handley, V.V. Kokorin, Appl. Phys. Lett. 69 (1996) 1966.
[2] M. Pasquale, C.P. Sasso, L.H. Lewis, L. Giudici, T. Lograsso, D. Schlagel, Phys. Rev. B 72 (2005) 094435.
[3] T. Krenke, M. Acet, E.F. Wassermann, X. Moya, L. Mañosa, A. Planes, Phys. Rev. B 72 (2005) 014412.
[4] T. Krenke, M. Acet, E.F. Wassermann, X. Moya, L. Mañosa, A. Planes, Phys. Rev. B 73 (2006) 174413.
[5] Mahmud Khan1, Igor Dubenko, Shane Stadler, Naushad Ali, J. Phys.: Condens. Matter 20 (2008) 235204.
[6] S. Stadler, M. Khan, J. Mitchell, N. Ali, I. Dubenko, A.Y. Takeuchi, A.P. Guimarães, Appl. Phys. Lett. 88 (2006) 192511.
[7] T. Krenke, E. Duman, M. Acet, E.F. Wassermann, X. Moya, L. Mañosa, A. Planes, Nat. Mater. 4 (2005) 450.
[8] X. Zhang, B. Zhang, S. Yu, Z. Liu, W. Xu, G. Liu, J. Chen, Z. Cao, G. Wu, Phys. Rev. B 76 (2007) 132403.
[9] M. Khan, N. Ali, S. Stadler, J. Appl. Phys. 101 (2007) 053919.
[10] A.K. Pathak, B.R. Gautam, I. Dubenko, M. Khan, S. Stadler, N Ali, J. Appl. Phys. 103 (2008) 07F315.
[11] B. Ingale, R. Gopalan, V. Chandrasekaran, S. Ram, J. Appl. Phys. 105 (2009) 023903.
[12] R. Kainuma, Y. Imano, W. Ito, Y. Sutou, H. Morito, S. Okamoto, O. Kitakami, K. Oikawa, A. Fujita, T. Kanomata, K. Ishida, Nature (London) 439 (2006) 957.
[13] H.S. Liu, C.L. Zhang, Z.D. Han, H.C. Xuan, D.H. Wang, Y.W. Du, J. Alloys Compd. 467 (2009) 27.
[14] B. Bao, Y. Long, J.F. Duan, P.J. Shi, G.H. Wu, R.C. Ye, Y.Q. Chang, J. Zhang, C.B. Rong, J. Appl. Phys. 103 (2008) 07B335.
[15] A.K. Nayak, K.G. Suresh, A.K. Nigam, J. Phys. D: Appl. Phys. 42 (2009) 035009.
[16] J. Du, Q.W. Zheng, J. Ren, W.J. Feng, X.G. Liu, Z.D. Zhang, J. Phys. D: Appl. Phys. 40 (2007) 5523.
[17] Y. Sutou, Y. Imano, N. Koeda, T. Omori, R. Kainuma, K. Ishida, K. Oikawa, Appl. Phys. Lett. 85 (2004) 4358.
[18] A.K. Nayak, K.G. Suresh, A.K. Nigam, J. Phys. D: Appl. Phys. 42 (2009) 115004.
[19] A.K. Nayak, K.G. Suresh, A.K. Nigam, J. Appl. Phys. 106 (2009) 053901.
[20] P.A. Bhobe, K.R. Priolkar, P.R. Sarode, J. Phys.: Condens. Matter 20 (2008) 015219.
[21] S. Chatterjee, S. Giri, S. Majumdar, S.K. De, Phys. Rev. B 77 (2008) 012404.